



Molecular Crystals and Liquid Crystals

Publication details, including instructions for authors and subscription information:

<http://www.tandfonline.com/loi/gmcl20>

Systematic Study of Absorption Spectra of Donor-Acceptor Azobenzene Mesogenic Structures

U. A. Hrozhyk^a, S. V. Serak^a, N. V. Tabiryan^a, L. Hoke^b, D. M. Steeves^b, B. Kimball^b & G. Kedziora^c

^a BEAM Engineering for Advanced Measurements Co., Winter Park, FL, USA

^b US Army Natick Soldier Research Development & Engineering Center, Natick, MA, USA

^c HPTi, HPCMP PET, OH, USA

Version of record first published: 05 Apr 2011

To cite this article: U. A. Hrozhyk, S. V. Serak, N. V. Tabiryan, L. Hoke, D. M. Steeves, B. Kimball & G. Kedziora (2008): Systematic Study of Absorption Spectra of Donor-Acceptor Azobenzene Mesogenic Structures, *Molecular Crystals and Liquid Crystals*, 489:1, 257/[583]-272/[598]

To link to this article: <http://dx.doi.org/10.1080/15421400802218959>

PLEASE SCROLL DOWN FOR ARTICLE

Full terms and conditions of use: <http://www.tandfonline.com/page/terms-and-conditions>

This article may be used for research, teaching, and private study purposes. Any substantial or systematic reproduction, redistribution, reselling, loan,

sub-licensing, systematic supply, or distribution in any form to anyone is expressly forbidden.

The publisher does not give any warranty express or implied or make any representation that the contents will be complete or accurate or up to date. The accuracy of any instructions, formulae, and drug doses should be independently verified with primary sources. The publisher shall not be liable for any loss, actions, claims, proceedings, demand, or costs or damages whatsoever or howsoever caused arising directly or indirectly in connection with or arising out of the use of this material.



Systematic Study of Absorption Spectra of Donor–Acceptor Azobenzene Mesogenic Structures

U. A. Hrozhyk¹, S. V. Serak¹, N. V. Tabiryan¹, L. Hoke²,
D. M. Steeves², B. Kimball², and G. Kedziora³

¹BEAM Engineering for Advanced Measurements Co., Winter Park, FL, USA

²US Army Natick Soldier Research Development & Engineering Center, Natick, MA, USA

³HPTi, HPCMP PET, OH, USA

The study reported herein is focused on measuring, as well as on modeling numerically, the positions and intensities of the absorption bands in the electronic spectrum of benzene ring-based mono-azo dyes, while preserving their potential mesogenic ability. Both non-polar structures, as well as highly polar push-pull structures, of azo dye molecules were designed and studied.

Keywords: azobenzene; liquid crystals; molecular design; UV-VIS spectrum

1. INTRODUCTION

Azobenzene-based liquid crystalline (LC) materials have been the focus of many studies because of their potential applications in modern photonic technologies. The reason for their popularity is the ability of azo compounds to reversibly change their shape upon illumination by light (photoisomerization) resulting in strong changes of the optical properties of the materials. Azo chromophores are considered to be in one of three spectral classifications depending on the energetic ordering and appearance of the π - π^* and n - π^* bands [1]. These are

This work was supported by the contract W911QY-07-C-0032. The authors gratefully acknowledge the DoD high performance computer ASC/MSRC resources to accomplish this work.

Address correspondence to Nelson Tabiryan, Beam Engineering for Advanced Measurements Co., 809, S. Orlando Ave., Suite I, Winter Park, FL, 32789, USA. E-mail: nelson@beamco.com.; U. A. Hrozhyk, Beam Engineering for Advanced Measurements Co., 809 S. Orlando Ave., Suite I, Winter Park, FL, 32789, USA. E-mail: uladzimir@beamco.com

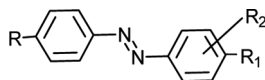
the “azobenzene” type, the “aminoazobenzene” type and the “pseudo-stilbene” type. “Azobenzene” type molecules possess a low intensity $n-\pi^*$ absorption band in the visible region and a high-intensity $\pi-\pi^*$ band in the UV region. Electron donating group substitutions on the benzene ring such as $-\text{NH}_2$ lead to the “aminoazobenzene” type where the $n-\pi^*$ and $\pi-\pi^*$ bands are very close together or overlapping in the violet or near UV region. In the “pseudo-stilbene” azos, with the substitutions of push/pull electron donor and electron acceptor pairs, the $\pi-\pi^*$ band appears in the visible range with an $n-\pi^*$ band in the UV. Typically azo LCs are of the “azobenzene” type. Expanding the absorption range, i.e., obtaining azo LCs with a red shifted $\pi-\pi^*$ band, would be very helpful for increasing their photosensitivity to visible electromagnetic radiation and broadening their application potential.

Azo compounds are the largest class of industrially synthesized organic dyes, and the absorption bands of azo dyes intended for coloring technologies cover the entire visible spectrum. However, these dye molecules are based on structures that are too cumbersome, or have other features that are prohibitive for the formation of a liquid crystalline phase. Use of such non-mesogenic azo dyes in mixtures with azo LCs for broadening of their absorption range is very limited due to the poor solubility of non-mesogenic azo dyes in LC media. Since the orientational order of LC materials stays high in the presence of mesogenic azo dopants, the effect of their photoisomerization on the material can be expected to be stronger than that of non-mesogenic dopants.

In this paper we have carried out a systematic study of the wavelength domain of the visible spectrum that can be covered by the absorption bands of benzene rings-based mono azo dyes possessing potential mesogenicity. The molecules based on such low molecular weight structures usually form substances with relatively low melting points. This consideration is the second significant circumstance from a practical point of view; low molecular weight mesogenic azo compounds are preferred as components of azo LC compositions with a practically useful temperature range.

2. RESULTS AND DISCUSSION

We studied the position of absorption bands in the UV-VIS spectrum of benzene rings-based mono-azo dyes, represented by the formula depicted below:



varying the chemical origin of terminal pendants R and R₁, and sometimes inserting additional lateral electron withdrawing pendants R₂, aimed at varying their peak absorption wavelength while preserving potential mesogenic ability. Over 30 molecular structures were synthesized, tested, and modeled numerically. The molecules studied include non-polar structures as well as highly polar ones in which the electron-donating and electron-withdrawing groups are placed on the opposite ends of the azobenzene core (push-pull structures).

Such R substituents as alkyl, -C_nH_{2n+1}; alkoxy, -OC_nH_{2n+1}; alkylthio, -SCH₃; dimethylamino, -N(CH₃)₂; and ethylpiperazinyl, -N(CH₂)₄N-C₂H₅ were chosen as electron donor pendants. R₁ consisted of alkyl, -C_nH_{2n+1}; alkoxy, -OC_nH_{2n+1}; and electron acceptor groups such as cyano, -CN; nitro, -NO₂; fluoro, -F; trifluoromethyl, -CF₃; trifluoromethoxy, -OCF₃; and isothiocyanato, -NCS groups. Mesogenic ability of azobenzene derivatives is well-recognized and there are mesogenic molecules incorporating lateral acceptor pendants that are not very bulky [2,3]. We can assume therefore that the presence of small lateral pendants in azobenzene structures should not appreciably affect the mesogenic ability of azobenzene derivatives.

As can be seen from Table 1, the experimentally obtained maxima λ_{max}^{exp} of the π - π^* absorption bands of the azobenzenes studied range between 334 (C4-azo-CF₃) [9] and 483 nm (C2N-azo-NO₂) [21]. (The azobenzene dyes listed in Table 1 are each labeled by a bold number in square brackets.) Electronic spectra were recorded with an Ocean Optics UV-VIS spectrometer for dye solutions in chloroform at 2×10^{-5} mol · l⁻¹ concentration. Melting points and phase transition points shown in Table 1 were determined with a polarizing microscope equipped with a thermo stage or in an open capillary. All phase transition points are uncorrected.

Table 1 allows comparison of these experimental values with the results of density functional theory (DFT) predictions. Figure 1 allows a visual comparison of the absorption bands of some of the azo dyes studied and Figure 2 provides a graphic comparison of the experimentally measured absorption bands and the DFT predicted absorptions. The molar extinction coefficients of these dyes are in the range 17,000 to 37,000 L · mol⁻¹ · cm⁻¹. This spectral range appears to set the limits of π - π^* absorption band positions for potentially mesogenic azo dyes designed as simple structures on the basis of only two benzene rings. These limits may vary due to the solvatochromic effect in different solvents. The absorption bands of these materials will be further shifted towards red in liquid crystalline compounds due to their high polarity.

The structures possessing the shortest wavelength absorption include those based on alkyl pendants R even if the opposite end of

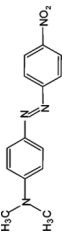
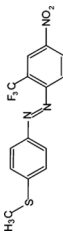
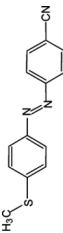
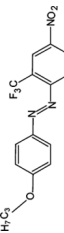
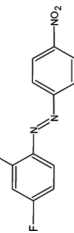
TABLE 1 Measured and Calculated Maxima of π - π^* Absorption Bands (λ_{max} , nm) of Several Azo Dyes and Their Thermal Properties

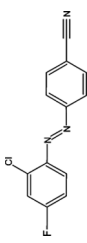
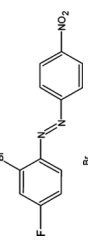
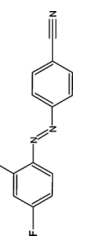
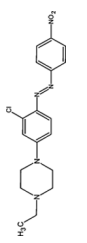
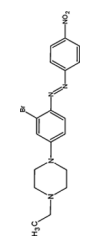
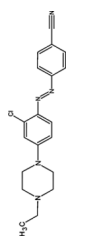
[Dye No.] Code Chemical name	Structural formula	Phase transitions, °C	$\lambda_{\text{trans}}^{\text{calc}}$ (nm)	$\lambda_{\text{cis}}^{\text{calc}}$ (nm)	$\lambda_{\text{max}}^{\text{exp}}$ (nm)
[1] C4-azo-OC1 4-Butyl-4'-methoxyazobenzene		32-nematic-48	474 (0.00)	490 (0.06)	352
[2] C4-azo-C1 4-Butyl-4'-methylazobenzene		m.p. 52	359 (1.01)	320 (0.17)	338
[3] C6-azo-CN 4-Cyano-4'-hexylazobenzene		m.p. 89- [*] [72.5] nematic	481 (0.00)	488 (0.05)	345
[4] C6O-azo-CN 4-Cyano-4'-hexyloxyazobenzene		99-nematic-116.5	344 (1.04)	308 (0.15)	373
[5] C4-azo-NO2 4-Butyl-4'-nitroazobenzene		m.p. 74	502 (0.00)	494 (0.06)	358
[6] C4O-azo-NO2 4-Butoxy-4'-nitroazobenzene		m.p. 111	356 (1.15)	316 (0.17)	384
[7] C4-azo-F 4-Butyl-4'-fluoroazobenzene		m.p. 43	495 (0.00)	495 (0.08)	337
[8] C4O-azo-F 4-Butoxy-4'-fluoroazobenzene		m.p. 80- [*] [63] nematic	377 (1.10)	334 (0.23)	355
[9] C4-azo-CF3 4-Butyl-4'-trifluoromethylazobenzene		m.p. 56- [*] [48] smectic, not identified	518 (0.00)	502 (0.07)	334
[10] C4O-azo-CF3 4-Butoxy-4'-trifluoromethylazobenzene		m.p. 103- [*] [88] smectic, not identified	372 (0.98)	358 (0.09)	356
[11] C4-azo-OCF3 4-Butyl-4'-trifluoromethoxyazobenzene		m.p. 43- [*] [41] smectic, not identified	511 (0.00)	502 (0.09)	337

[12] C4O-azo-OCF ₃ 4-Butoxy-4'-trifluoromethoxyazobenzene		82-smectic A-106	476 (0.00) 360 (0.98)	487 (0.06) 323 (0.22)	354
[13] C4-azo-3F 4-Butyl-2',4',6'-trifluoroazobenzene		m.p. 26	499 (0.00) 341 (0.98)	464 (0.05) 305 (0.02)	349
[14] C4O-azo-3F 4-Butoxy-2',4',6'-trifluoroazobenzene		m.p. 46	491 (0.00) 359 (0.94)	468 (0.06) 322 (0.22)	352
[15] C4-azo-2F 4-Butyl-2',4'-difluoroazobenzene		m.p. 39	491 (0.00) 337 (0.99)	475 (0.05) 307 (0.04)	342
[16] C4-azo-FCF ₃ 4-Butyl-4'-fluoro-2'-(trifluoromethyl)azobenzene		m.p. 32	485 (0.01) 337 (0.88)	476 (0.05) 307 (0.19)	340
[17] C4-azo-4FCN 4-Butyl-4'-cyano-2',3',5',6'-tetrafluoroazobenzene		m.p. 54	515 (0.02) 357 (1.02)	469 (0.07) 324 (0.08)	344
[18] S-azo-NO ₂ 4-Methylthio-4'-nitroazobenzene		m.p. above 120	516 (0.00) 429 (0.80)	511 (0.11) 397 (0.09)	406
[19] S-azo-OCF ₃ 4-Methylthio-4'-trifluoromethoxyazobenzene		m.p. 102- [*] [98] smectic, not identified	482 (0.00) 386 (0.86)	494 (0.07) 352 (0.18)	373
[20] C2N-azo-NCS 4-Dimethylamino-4'-isothiocyanatoazobenzene (Aldrich)		m.p. 167	482 (0.00) 420 (1.38)	508 (0.15) 366 (0.26)	444

(Continued)

TABLE 1 Continued

[Dye No.] Code Chemical name	Structural formula	Phase transitions, °C	λ_{trans}^{calc} (nm)	λ_{cis}^{calc} (nm)	λ_{max}^{exp} (nm)
[21] C2N-azo-NO2 4-Dimethylamino- 4'-nitroazobenzene		—	509 (0.00) 444 (0.91)	512 (0.15) 415 (0.07)	483
[22] S-azo-CF3NO2 4-Methylthio-4'-nitro- 2-trifluoromethyl azobenzene		m.p. 142	518 (0.00) 418 (0.85)	505 (0.12) 407 (0.06)	421
[23] S-azo-CN 4-Methylthio- 4'-cyanoazobenzene		m.p. 157	501 (0.00) 405 (0.92)	502 (0.09) 365 (0.19)	391
[24] C3O-azo-CF3NO2 4-Propyloxy-4'-nitro- 2'-trifluoromethyl azobenzene		m.p. above 120	512 (0.00) 387 (0.97)	496 (0.10) 383 (0.09)	398
[25] 4F-2Cl-azo-NO2 2-Chloro- 4-fluoro-4'-nitroazobenzene		m.p. 114	544 (0.01) 356 (0.71)	496 (0.06) 348 (0.07)	353

[26] 4F-2Cl-azo-CN 2-Chloro-4-fluoro-4'-cyanoazobenzene		m.p. 126	528 (0.01) 345 (0.82)	489 (0.06) 322 (0.04)	342
[27] 4F-2Br-azo-NO2 2-Bromo-4-fluoro-4'-nitroazobenzene		m.p. 110	527 (0.00) 376 (0.58)	480 (0.05) 348 (0.02)	350
[28] 4F-2Br-azo-CN 2-Bromo-4-fluoro-4'-cyanoazobenzene		m.p. above 150	538 (0.01) 352 (0.59)	472 (0.04) 331 (0.01)	348
[29] CPND-2 1-(2-Chloro-4-N-ethylpiperazinyl)-phenyl)-2-(4-nitrophenyl)-diazene		m.p. 130	547 (0.00) 431 (0.90)	545 (0.11) 421 (0.01)	422
[30] BPND-2 1-(2-Bromo-4-N-ethylpiperazinylphenyl)-2-(4-nitrophenyl)diazene		m.p. 150	558 (0.00) 431 (0.94)	554 (0.12) 426 (0.01)	422
[31] CPCD-2 1-(2-Chloro-4-N-ethylpiperazinylphenyl)-2-(4cyanophenyl)diazene		m.p. 138	529 (0.00) 404 (1.12)	530 (0.12) 395 (0.06)	408

* {} – Phase transition is monotropic.

Note: Predicted oscillator strengths for a transition are provided in parenthesis following the transition wavelength.

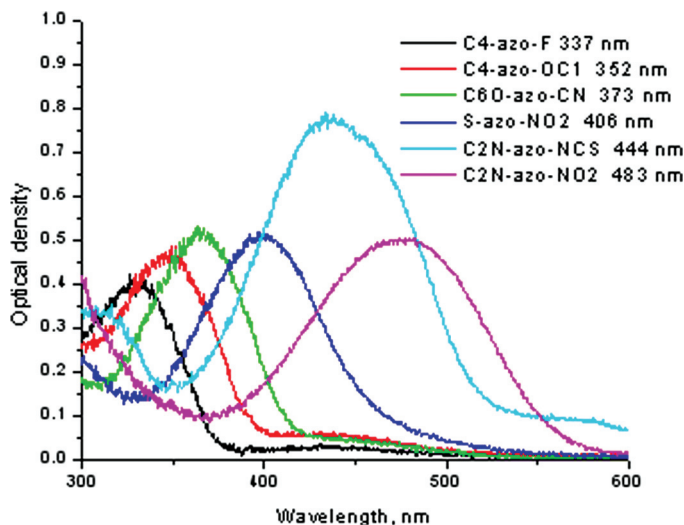


FIGURE 1 UV-VIS spectra of several azo dyes.

the azobenzene core is occupied by such acceptor groups R_1 as -F, -CF₃, -OCF₃, and -CN. Even the presence of the second similar group R_2 in the acceptor part of the molecule does not shift the absorption band towards the red. Only such a strong acceptor as the -NO₂ group is able to counteract the alkyl pendant. The replacement of the alkyl

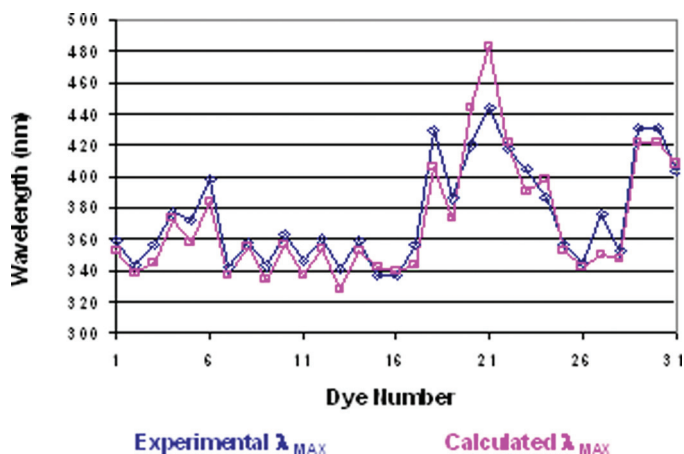


FIGURE 2 Comparison of experimental and calculated λ_{MAX} . Experimental solvent is chloroform compared to molecular modeling predictions for single isolated azobenzene dye molecules.

group by the alkoxy pendant and, what is more, by the thioalkyl pendant, causes a red shift of the absorption bands.

The red shift of the π - π^* band maximum caused by alkoxy pendants against alkyl ones is from 14 nm (the pairs $\text{CH}_3\text{O}/\text{C}_4\text{H}_9$ [1] and $\text{CH}_3/\text{C}_4\text{H}_9$ [2]) to 28 nm (the pairs $\text{C}_6\text{H}_{13}\text{O}/\text{CN}$ [4] and $\text{C}_6\text{H}_{13}/\text{CN}$ [3]). Replacement of O by S leads up to a 23 nm additional red shift (the pairs $\text{CH}_3\text{S}/\text{OCF}_3$ [19] and $\text{C}_4\text{H}_9\text{O}/\text{OCF}_3$ [12], $\text{CH}_3\text{S}/\text{NO}_2$ [18] and $\text{C}_4\text{H}_9\text{O}/\text{NO}_2$ [6], $\text{CH}_3\text{S}/\text{CF}_3\text{NO}_2$ [22] and $\text{C}_3\text{H}_7\text{O}/\text{CF}_3\text{NO}_2$ [24], $\text{CH}_3\text{S}/\text{CN}$ [23] and $\text{C}_6\text{H}_{13}\text{O}/\text{CN}$ [4]).

It is interesting that the presence of a single lateral acceptor substituent such as -F and, especially, $-\text{CF}_3$ in the *o*-position relative to the $-\text{N}=\text{N}-$ bond leads to an appreciable bathochromic shift of an absorption band. The pair $\text{C}_4\text{H}_9/2\text{F}$ [15] vs. the pair $\text{C}_4\text{H}_9/\text{F}$ [7] is bathochromically shifted only by 5 nm, whereas the bathochromic shifts of the pairs $\text{C}_4\text{H}_9/\text{FCF}_3$ [16] vs. $\text{C}_4\text{H}_9/\text{F}$ [7], $\text{C}_3\text{H}_7\text{O}/\text{CF}_3\text{NO}_2$ [24] vs. $\text{C}_4\text{H}_9\text{O}/\text{NO}_2$ [6], and $\text{S}/\text{CF}_3\text{NO}_2$ [22] vs. S/NO_2 [18] are 3, 14, and 15 nm, respectively. In contrast, the increase of the acceptor -F substituents leads to hypsochromic shifts; compare the pairs $\text{C}_4\text{H}_9/\text{F}$ [7] vs. $\text{C}_4\text{H}_9/3\text{F}$ [13] (12 nm hypsochromic shift) and $\text{C}_4\text{H}_9/4\text{FCN}$ [17] vs. $\text{C}_6\text{H}_{13}/\text{CN}$ [3] (1 nm hypsochromic shift).

Also it is interesting to note that the presence of electron withdrawing halogens Cl and Br instead of an electron donating alkyl group R in the structures with $\text{R}_1 = -\text{CN}$ leads to a bathochromic shift. The shift of the absorption band for 4F-2Br-azo- NO_2 [27] vs. $\text{C}_4\text{H}_9/\text{NO}_2$ [5] is slightly hypsochromic, see Table 1. This observation can be explained by attributing halogens a dual role in electron distribution in the aromatic molecules; possessing electron negativity they can serve at the same time as electron donor pendants in the presence of strong acceptors R_1 due to participation of their nonbonding electrons [4].

The presence of nitrogen (as amine group nitrogen) in the electron donor part of the azo dye molecule simultaneously with the presence of electron acceptor groups $-\text{NO}_2$ and $-\text{NCS}$ leads to a significant red shift of the maximum of the π - π^* band (azodyes incorporating $(\text{CH}_3)_2\text{N}/\text{NO}_2$ [21] and $(\text{CH}_3)_2\text{N}/\text{NCS}$ [20] pairs). The largest red shifted spectra were observed for 4-dimethylamino-4'-isothiocyanatoazobenzene and 4-dimethylamino-4'-nitroazobenzene with maxima at 444 and 483 nm. Replacement of R_2N by an N-ethylpiperazinyl pendant causes a smaller red shift.

The donor-amino and acceptor-nitro pair induces the strongest red shift of the absorption band in the azobenzene molecules. This fact has theoretical confirmation. The absorption maximum shifts towards longer wavelengths with increasing strength of the donor and the acceptor. The strength of accepting and donating properties of the

pendants can be estimated by the value of Hammett's substituent constant $|\sigma|$ [5]. The values of $|\sigma|$ for tertiary amino group $>\text{N}-$ and nitro group $-\text{NO}_2$ are 0.83 and 0.78, respectively. For comparison, the values of $|\sigma|$ for alkoxy group $\text{RO}-$ and cyano group $-\text{CN}$ are 0.27 and in the range 0.63–1.00, respectively [6–8]. The sums of the values $|\sigma|$ are the largest for the tertiary amino group–nitro group and tertiary amino group–cyano group pairs. The values of $|\sigma|$ for other accepting groups are considerably smaller; for example $|\sigma| = 0.54$ for the $-\text{CF}_3$ group.

Mulliken charges on various prototypical azos are shown in Figure 3. For the 4-dimethylamino-4'-nitroazobenzene molecule [21], we see that the amino nitrogen has a negative charge and the nitro nitrogen has a positive charge, which is a consequence of their electron donor and acceptor characteristics, respectively. Note the relative charges of the carbons at the 1, 1', 4, and 4' positions. For [21], those carbons have a positive charge at all four positions unlike the other molecules. A study of the correlation between the charges on the atoms and the absorption energy of the $\pi-\pi^*$ band revealed that the charge difference between the 1 and 1' carbons and their neighboring nitrogens is well correlated to the absorption energy. The greater the average charge difference between the two paired nitrogen-carbon charges, the lower the energy of the $\pi-\pi^*$ band. These qualitative characteristics provide us a method to narrow the search for molecules possessing lower energy $\pi-\pi^*$ absorption energies.

Note that almost half of the compounds studied here possess mesogenicity; in most cases their mesophases are monotropic and smectic (see Table 1). Most of the homologs of C4-azo-C1 [2] and some of the

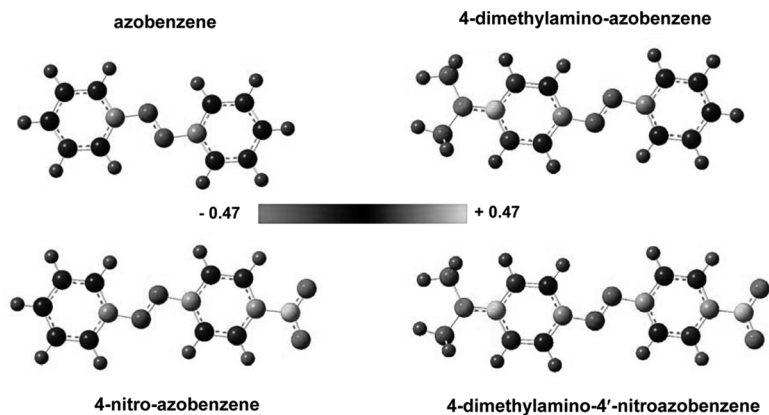


FIGURE 3 Atomic Mulliken charges of different types of azo molecules.

4-alkoxy-4'-nitroazobenzenes [9] are nematics. The ability of 11 out of 25 potentially mesogenic compounds to form mesophases confirms the potentially high mesogenic ability of these azobenzene derivatives.

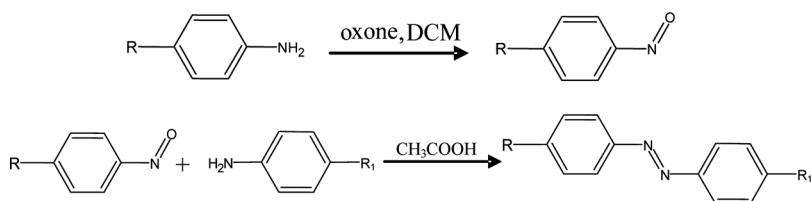
The mesogenic ability of homologs of such azo dyes as C4-azo-OC1 [1], C4-azo-C1 [2], C6-azo-CN [3], C6O-azo-CN [4] has been studied before [10,11]. Such dyes as C4O-azo-F [8], C4-azo-CF₃ [9], C4O-azo-CF₃ [10], C4-azo-OCF₃ [11], C4O-azo-OCF₃ [12], and S-azo-OCF₃ [19] could serve as future candidates for the study of mesogenic ability in their homologous series. For mesogenic azo dyes intended for long wavelength absorption we can consider only structures based on RS- and R₂N- electron donor pendants.

A practical disadvantage of the azo compounds based on push-pull structures is that they have, as a rule, high melting points due to the presence of groups with high local dipole moments (3.3 Debye for -CN, 2 Debye for -NCS). However, a wide choice of suitable molecules that can be designed based on the proposed structures should allow the development of multicomponent mixtures possessing suitable thermal and optical properties. Such compositions unavoidably require the presence of lower melting components even if they do not have absorption at suitable wavelengths. Low melting azobenzenes with fluorinated terminals, provided nematic homologs can be found among them, may be useful for development of room temperature compositions because they may have better miscibility with polar azo components than azobenzenes with non-polar molecules.

3. SYNTHESIS

Usually, azo dyes are obtained through the reaction of azo coupling of diazotized aromatic amines with phenols or amines and subsequent modification of hydroxy- or aminoazobenzenes. However, such azo compounds as dialkyl azobenzenes cannot be obtained through the reaction of azo coupling. Therefore, the reaction of aromatic C-nitroso compounds with aromatic amines was used for obtaining most of the azo dyes in this study.

The schematic of the two step reaction is depicted below:



The typical protocol of the syntheses is described below. All chemicals and solvents were purchased from Sigma-Aldrich and used without purification.

3.1. C-Nitroso Derivatives

R-substituted aniline (10 mmol) was dissolved in a sufficient volume of dichloromethane (DCM). Oxone (12.3 g, 20 mmol), dissolved in 100 mL of water, was added to this solution. The reaction mixture, depending on the specific compound, was stirred for 2 to 72 h at 0°C or at room temperature. After separation of the layers, the aqueous layer was twice extracted with DCM. The combined green colored organic layers were washed with 1 N HCl, saturated sodium bicarbonate, water, and brine, and dried over anhydrous sodium sulfate. After filtering and removal of the solvent the pale yellow or light green solid or dark green liquid product was used further without purification.

3.2. Azo Dyes

The nitroso derivative obtained from the appropriate aniline in the previous step was dissolved (sometimes not totally if the nitroso compound was a solid powder) in 60 mL of glacial acetic acid. To this green solution (or light-green suspension) R₁-substituted aniline (12 mmol) was added. The reaction mixture was stirred at room temperature overnight. Then it was diluted with 200 mL of 2% aqueous NaCl and 150 mL of DCM was added. The organic layer was separated and the water layer was extracted with DCM (2 × 40 mL). The combined organic layer was washed with water, saturated sodium bicarbonate, water, brine, and dried over anhydrous sodium sulfate. After removal of the solvent with a rotary evaporator the product was purified by column chromatography (silica gel, the eluents used, viz. DCM, ethyl acetate, and acetone). Final yields of the products were in the 6 to 70% range.

Attempts to obtain two of the azo dyes, 4-butyl-4'-fluoro-2'-nitroazobenzene and 4-butyl-4'-cyano-2'-nitroazobenzene, were unsuccessful due to the high solubility of the starting nitroanilines in water. The reaction of formation of the nitroso compounds proceeds on the interphase boundary between the organic and water layers; therefore, high solubility of the starting compound in water obstructs this reaction. Surprisingly, the reverse reaction of these 2-nitroaniline derivatives with the test nitroso compound, 4-ethyl-4'-nitrosoazobenzene, also was unsuccessful. This is likely to be caused by the presence of such

a bulky substituent as the $-\text{NO}_2$ group in the *ortho*-position that creates strong steric hindrance for the coupling reaction. The reaction of anilines with *ortho*-substituted di-fluoro or trifluoromethyl nitroso compounds occurs easily. Such obstruction as the presence of intramolecular H-bonds in *ortho*-nitroanilines [12] seems to be less probable because intramolecular H-bonds most likely are transformed into intermolecular H-bonds in a protic solvent such as acetic acid. This reaction of obtaining azo compounds through nitroso derivatives, straightforward in many cases, needs further study and improvement.

4. MODELING

Geometry optimizations were conducted for all dyes for both the *trans* and *cis* isomers using the B3LYP/6-31G* method and basis set. UV/VIS absorptions and oscillator strengths were predicted for single isolated molecules based on the optimized geometries using time-dependent density functional theory TD-DFT. These calculations and the Mulliken charge calculations were performed with the Gaussian 03 electronic structure program [13]. The wavelengths for the first two vertical

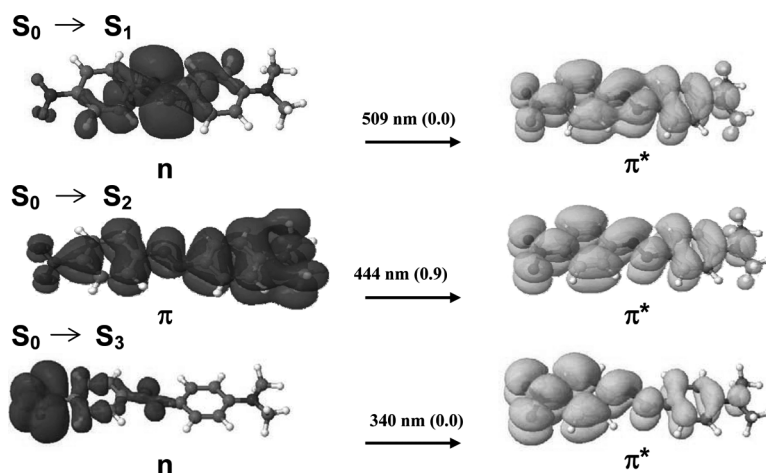


FIGURE 4 Electron attachment–detachment plots of 4-dimethylamino-4'-nitroazobenzene [21] with theoretical excitation wavelength and oscillator strengths in parentheses. The isosurface on the left represents the electron density that is removed from the ground state (detachment), and the isosurface on the right represents that electron density (attached) in the excited state.

transitions for both the *trans* and *cis* isomers are provided in Table 1 along with the associated oscillator strengths for each transition. The longest wavelength predicted transition for the *trans* isomers have a very small or zero oscillator strength suggesting that this corresponds to an $n\text{-}\pi^*$ type transition. The next *trans* isomer transition for each dye is strong with a large oscillator strength suggesting a $\pi\text{-}\pi^*$ type transition. This transition was compared to the experimentally measured λ_{max} values. TD-DFT electron attachment-detachment plots [14,15] support these assignments. Figure 4 shows such plots for the three lowest singlet transitions of C2N-azo-NO2 [21]. In additional cases where electron attachment-detachment plots were made, there is an $n\text{-}\pi^*$ transition with zero oscillator strength lower in energy than the $\pi\text{-}\pi^*$ transition with a large oscillator strength. Based on the comparison of the calculation with the experimental results, the contribution of the *cis* form of the dyes to the spectra is quite small and perhaps only noticeable in the $n\text{-}\pi^*$ bands.

A graphical comparison of the theoretically estimated and experimentally measured band peaks is provided in Figure 2. The UV/VIS absorptions for the dye 4-dimethylamino-4'-nitroazobenzene have been studied with quantum chemical methods by Poprawa-Smoluch et al. [16] and our results reported here for *trans* and *cis* isomer absorption wavelengths and oscillator strengths for this azobenzene dye are in agreement. The difficulty for TD-DFT to accurately reproduce excitation energies with significant charge transfer is well known and may be improved with newer functionals. However, for the trends we observe in this work using the B3LYP functional is adequate.

Additional calculations of the electronic excitation energies and oscillator strengths of azobenzene and amino azobenzene show a low-energy dark $n\text{-}\pi^*$ excitation exists in agreement with those molecules included in Table 1. In the case of azobenzene, this band is observed [1] even though the absorption is not electronically dipole allowed as shown by the theoretical calculations. For C2N-azo-NO2 [21], the $n\text{-}\pi^*$ S1 band is close in energy to the $\pi\text{-}\pi^*$ S2 band, and it is not observed as a separate band. The S3 $n\text{-}\pi^*$ band shown in the electron attachment-detachment chart (Fig. 4), accounts for the experimentally observed UV band. Note that it is not a change in the order of the orbitals or even a change in the order of the states relative to the azobenzene ordering that accounts for the observed high-energy $n\text{-}\pi^*$ band [1], but rather the reasons are more complex and likely have to do with vibronic interactions, which are not included in the theoretical calculations, or contributions from *cis* azo conformations.

5. SUMMARY

This study suggests specific principles for designing mesogenic azo dyes with absorption bands covering a wide spectral range. The potentially mesogenic azo dyes under investigation exhibit π - π^* absorption bands in the spectral range between 334 and 483 nm in chloroform. The ability of 11 out of 25 of the compounds studied to form mesophases indicates high mesogenic ability of the azobenzene derivatives. For mesogenic azo dyes intended for longer wavelength absorption the push-pull structures based on alkylthio and alkylamino as donor pendants and isothiocyanato and nitro groups as acceptor pendants appears to be most useful.

Molecular modeling predictions provided good agreement with experimentally measured trends when comparing the absorption bands of the azobenzene dyes evaluated here as shown in Figure 2.

Structures such as 4-alkyl(alkyloxy)-4'-fluoroazobenzenes, 4-alkyl(alkyloxy)-4'-trifluoroazobenzenes, 4-alkyl(alkyloxy)-4'-trifluoromethoxyazobenzenes, 4-alkylthio-4'-trifluoromethoxyazobenzenes are candidates for the future study of mesogenic ability in their homologous series to obtain low melting polar LC azo dyes. The results suggest that further progress in red shifting of the absorption bands of mesogenic azo dyes can be achieved with structures containing hetaryl moieties replacing benzene rings. It should be expected that such structures will be more bathochromic than the corresponding non-hetarylazo derivatives.

REFERENCES

- [1] Rau, H. (1990). Photoisomerization of azobenzenes In: *Photochemistry and Photo-physics*, Rabeck, J. F. (Ed.), CRC Press: Boca Raton, FL, Chapter 2, 119.
- [2] Kelly, S. M. & O'Neill, M. (2000). Liquid Crystals for Electro-Optic Applications In: *Handbook of Advanced Electronic and Photonic Materials and Devices*, Nalwa, H. S. (Ed.), Academic Press: Japan, Volume 7, Chapter 1.
- [3] Petrov, V. F. (2001). *Liquid Crystals*, 28, 217.
- [4] McMurry, J. E. (1992). *Organic Chemistry*, Brooks Cole: Pacific Grove, CA.
- [5] Hammett, L. P. (1937). *J. Amer. Chem. Soc.*, 59, 96.
- [6] Wiberg, K. (1964). *Physical Organic Chemistry*, John Wiley and Sons: New York, NY.
- [7] Maskill, H. (1989). *The Physical Basis of Organic Chemistry*, Oxford University Press: Oxford, England.
- [8] Lowry, T. & Richardson, K. S. (1987). *Mechanism and Theory in Organic Chemistry*, Harper and Row: New York, NY.
- [9] Tsutsumi, O., Kanazawa, A., Shiono, T., Ikeda, T., & Park, L.-S. (1999). *Phys. Chem. Chem. Phys.*, 1, 4219.
- [10] Steinsträsser, R. & Pohl, L. (1971). *Zeit. für Naturforsch.*, 26b, 577.

- [11] Hrozhyk, U., Serak, S., Tabiryan, N., & Bunning, T. J. (2006). *Mol. Cryst. Liq. Cryst.*, 454, 243.
- [12] Krueger, P. J. (1963). *Can. J. Chem.*, 41, 363.
- [13] Frisch, M. J., et al. (2004). *Gaussian 03, Revision D.02.*, Gaussian, Inc.: Wallingford, CT.
- [14] Head-Gordon, M., Graña, A. M., Maurice, D., & White, C. A. (1995). *J. Phys. Chem.*, 99, 14261.
- [15] Shao, Y., et al. (2006). *Phys. Chem. Chem. Phys.*, 8, 3172.
- [16] Poprawa-Smoluch, M., et al. (2006). *J. Phys. Chem. A*, 110, 11926.